Expanded percolation theory model for the temperature induced forming (TIF) of alumina aqueous suspensions

Yunpeng Yang, Wolfgang M. Sigmund*

Department of Materials Science and Engineering, 225 Rhines Hall, University of Florida, Gainesville, FL 32611-6400, USA

Abstract

A continuous percolation model is proposed to describe the temperature and volume fraction dependence of the shear modulus of temperature induced forming (TIF) alumina aqueous suspensions. The concept of "effective volume fraction of aggregates" is proposed. The volume fraction gelation threshold (ϕ_g), the characteristic temperature (T_0) and the exponent (s) can be derived from the rheological measurements. Model calculations are in good agreement with the measurement data. The estimation of the strength of the wet gelled alumina suspensions with variation in temperature can be realized using this model. © 2002 Elsevier Science Ltd. All rights reserved.

Keywords: Al$_2$O$_3$; Colloidal processing; Gelation threshold; Percolation model; Shear modulus; Temperature induced forming

1. Introduction

Industrial application needs a ceramic forming method that has a high reliability as well as a simple process.[1] Colloidal processing has been realized to be useful for forming ceramic green bodies because of its capability to reduce the strength-limiting defects compared with the dry powder compaction processing.[2] Among the forming methods that utilize colloidal processing, direct casting methods attract more attention because of the constant volume during ceramic forming compared to the drain casting techniques.[3] Temperature induced forming (TIF) is a novel direct casting method through colloidal processing to form ceramic green bodies. A smaller molecular weight dispersant (i.e. ammonium citrate) and a larger molecular weight polymer (i.e. polyacrylic acid) are used to form stable concentrated aqueous suspensions at room temperature. The weight ratio of the organic additives to that of the ceramic powder is less than 0.5%. The suspensions can be induced to form bridging flocculation by the increasing dissolution of ceramic particles with temperature.[3–6]

Several processing parameters affect the rheological properties of the TIF suspensions, such as volume fraction of solids, dispersant amount, molecular weight of PAA, and pH of the resultant slurries, etc. It is also reported that aggregation will form flocs and grow in concentrated suspensions.[7]

The viscoelastic properties, in particular how the elastic modulus scales with volume fraction, have been modeled based on the assumption that the particle network consists of close packed flocs. Two models have been proposed to explain the experimental phenomena, fractal model and percolation model. The fractal models assume that suspensions can gel at all volume fractions; therefore, there is no gelation threshold. Several authors interpreted the elasticity of aggregated dispersions in terms of the fractal concept. The fractal models depend on the assumption that the aggregated structure transmits stress through its elastic backbone (a chain of particles). Fractal models of gelation predict that a space-filling network will be created when the characteristic floc size ξ is large enough that individual flocs overlap. In suspensions where a weak attraction causes slower aggregation and the aggregation is reaction limited, the viscoelastic properties, in particular how the elastic modulus scales with volume fraction, have been modeled based on the assumption that the particle network consists of close packed fractal flocs. The models predict

* Corresponding author. Tel.: +1-352-846-3343; fax: +1-352-392-7219.

E-mail address: wsigm@mse.ufl.edu (W.M. Sigmund).

a power law behavior of elastic modulus with respect to volume fraction

$$G' = G'_0 \cdot \phi^p \qquad (1)$$

where G_0 is the pre-exponential factor, ϕ is the volume fraction of clusters, and p is an exponent that relates to the structure through the fractal dimension of the flocs. P is about 4.5 for reaction limited cluster aggregation (RLCA).[8–11]

Percolation deals with the effects of varying the richness of interconnections present in a random system. The basic idea of percolation is the existence of a sharp transition at which the long-range connectivity of the system disappears or going the other way and appears. This transition occurs abruptly when some generalized density in this system reaches a critical value (percolation threshold). The models based on percolation concepts describe the importance of the gelation threshold ϕ_g to the rheological properties of aggregating suspensions. Rueb and Zukoski used an octadecyl silica/ethanol system to obtain a scaling for the storage modulus that follows:

$$G' = G'_0 (\phi/\phi_g - 1)^s \qquad (2)$$

where, the exponent, s is related to the microstructure of the network.[11,12] But experimental results of Yanez et al. on AKP-30 alumina/poly(12-hydroxy stearic acid)/hexanol system suggested that the expression $G' = G'_0 \cdot (\phi - \phi_g)^s$ captured the generic mechanical behavior of particle gels. Here, $\phi - \phi_g$ is the distance from the gel transition and thus relates to the number of stress carrying bonds. G'_0 characterizes the elasticity of the interparticle bonds, and which might be temperature dependent.[13] The power law dependence on shear modulus on volume fraction of particles has been documented often in the literature. Considering that the particle connectivity is very tortuous at all volume fractions so that many interpenetrating, percolative paths exist to support applied pressures at high volume fractions. For example, Sen et al. proposed a model for such a tortuous network and yielded $n = 4.4$.[14] During modeling, they changed the volume fraction of particles by randomly removing particles from a periodic array (face-centered cubic) of identical, spherical particles. The results of Yanez et al. showed that $n = 4.75 \pm 0.25$ for the attractive alumina particle networks in aqueous slurries.[15] Sonntag and Russel have found n to be 2.5 and 4.4 for fresh and aged polystyrene networks, respectively.[16] Shih et al. have experimentally determined that $n = 4.1$ for the modulus of agglomerated, platelike, boehmite alumina crystallites.[17] Buscall et al. have found $n = 4.3$ for the compressive yield stress of polystyrene latex systems aggregated with barium

chloride.[18] It is clear that these large values of n might be due to the percolative nature of particle networks.

Although the documented models predict that the modulus of the suspension increases with increasing volume fraction of the flocs, there are no reports on how to model the temperature dependence of the suspension modulus. Because temperature is an important parameter that will affect the suspension rheological properties, it is desirable for industrial application to get to know and control the variation of these properties with temperature. It is realized from the experimental results that the temperature dependence of the viscoelastic properties of the TIF suspensions shows "transition" behavior, i.e. gelation. Therefore, the authors think that the variation of the shear modulus with temperature for the TIF suspensions may be described using the percolation theory model if the percolative particle network forms. The following assumptions are proposed to evaluate the evolution of the microstructure of TIF suspensions at elevated temperatures.

2. Assumptions proposed for TIF alumina aqueous suspensions

1. Aggregate forms because of bridging flocculation in TIF suspensions, which arises from the interaction between particles and polymer chains at elevated temperature.
2. The number of aggregates formed is related to the magnitude of the EDL repulsive potential barrier, the initial volume fraction of particles and the amount of the polymer.
3. Viscoelastic properties, such as storage modulus and shear viscosity, increase with the number density of the stress carrying bonds in the aggregates, and the gelation of the slurry is due to the formation of the percolating particle network.
4. TIF alumina suspension has a volume fraction threshold, and above which the slurry can form a continuous filling network as the temperature is raised. This volume fraction threshold should vary with the molecular weight of PAA because the increasing possibility of the interactions between PAA chains and particles.
5. There is a critical temperature and above which the rheological behavior shows significant variations for the slurry whose solid volume fraction is above the gelation threshold. The origin of this critical temperature may relate to the balance of the thermal energy, the particle/PAA adsorption energy, van der Waals attraction potential and the EDL repulsive potential. This temperature may also vary with the molecular weight of PAA.
6. The size of aggregates grows with increasing temperature and a new concept, the "effective

volume fraction of aggregates", ϕ_{eff}, is introduced. Compared with the initial volume fraction of particle (ϕ_0), ϕ_{eff} increases at elevated temperatures because of the growth of the aggregates and which reaches maximum value of 1 in the completely gelled suspension. The concept of ϕ_{eff} can be thought as the total volume of the particles in an aggregate and the volume of the solvent trapped inside the backbone of the aggregate, and always $\phi_{\text{eff}} \geqslant \phi_0$.

3. Continuous percolation model

Considering the high order of stochastic geometry in concentrated suspensions so that the disorder-generating statistical variable (stable region/aggregates) is superimposed on a background structure that is itself topologically disorder (no lattice for aggregates positions), a continuous percolation can be realized. The whole system of high loading suspension has a two-fold disorder, statistical (for the state of aggregates to link to each other) and geometrical (for background structure). Adopting the similar form as Eq. (2) to relate the storage modulus with the volume fraction and temperature of the TIF alumina suspensions, Eq. (3) is proposed.

$$G'(T, \phi) = G'_0(T) \cdot \left[\phi_{\text{eff}}(T)/\phi_g - 1 \right]^s \quad (3)$$

Here, we use the "effective volume fraction of aggregates", ϕ_{eff}, instead of the initial volume fraction, ϕ_0, considering the formation and growth of the aggregates at elevated temperature. ϕ_g is the volume fraction gelation threshold. $G'_0(T)$ is a reflection of the strength of the aggregate backbone, which might vary with the molecular weight of polymer and the deviation from the thermal equilibrium condition. The exponent, s, is related to the microstructure of the network.[14–18]

Considering the intrinsic similarities (i.e. by thermal activation) between the formation and growth of the aggregate flocs in the TIF suspension, and the nucleation and growth of crystalline phase from solution, we propose that ϕ_{eff} may vary according to the following expressions.[19]

$$\phi_{\text{eff}}(T) = \phi_0 \cdot e^{-\Delta U/kT} \cdot F(\Delta T) \quad (4)$$

Where ϕ_0 is initial volume fraction of powders. ΔU is the total energy barrier to overcome for the formation of the aggregates at elevated temperature in the initially stable slurry. For the EDL stabilized alumina slurry, we fix $\Delta U = 5$ eV, which is corresponding to the value of the zeta potential of the alumina particles, ~ -60 mV at pH > 9.0. k is the Boltzmann constant. $F(\Delta T)$ is a function of the temperature T, which illustrates the effect of

the temperature on the growth of the aggregates. The authors propose the following expression for $F(\Delta T)$:

$$F(\Delta T) = e^{d1 \cdot [d2 + (T - T_0)/T_0]} \quad (5)$$

Then the final expression for the storage modulus is

$$G'(T, \phi_0) = G'_0 \cdot \left\{ \phi_0 \cdot e^{-\Delta U/kT} \cdot e^{d1 \cdot [d2 + (T - T_0)/T_0]} / \phi_g - 1 \right\}^s \quad (6)$$

where, $d1$ and $d2$ are constants, and their physical meanings are still under investigation. In the following calculations, we set $d1 = 1.3$ and $d2 = 0.1$ for the best fit of the experimental data. T_0 is the characteristic temperature where the bridging flocculates start to form for a molecular weight polymer containing slurry, and the value of T_0 is independent with the amount of polymer and volume fraction of particles. The values of ϕ_g, T_0, G'_0 and s can be estimated from the rheological measurements.

4. Slurry preparation and measurements

4.1. Raw materials

The raw materials and preparation of the suspensions are described as follows. The starting materials are AKP 53 α-alumina powder (Sumitomo, Japan), tri-ammonium citrate (TAC) powder (Aldrich, USA. 98%), and poly (acrylic acid) (PAA) (Polyscience, USA. 25 wt.% solutions in water, the average molecular weight is $\sim$5000, 10,000 and 50,000). The purity of α-Al$_2$O$_3$ powder is > 99.999% according to manufacturer. The particle size is measured by LS Particle Size Analyzer (COULTER) yielding $d_{50} = 0.45$ μm. The surface area of the alumina powder is measured by standard BET (NOVA 1200) N$_2$ adsorption giving 14.8 m^2/g. TAC powder is dissolvable in water and is used as dispersant. PAA is used here as a gelling agent, not a dispersant. Both the amount of TAC powder and PAA are based on the weight of dry alumina powders. The amount of TAC powder is fixed as 0.4 wt.%. The amount of PAA is taken as 0.04 wt.% because this is the minimum amount of PAA required to make the slurry gel.[20] At this small amount of PAA, the bridging flocculation by PAA has the high probability to be the main gelation mechanism.[21]

4.2. Preparation of the suspensions

The preparation of the suspensions is done with a planetary ball mill (Fritsch GMBH, Pulverisette 5, Germany. Alumina mill jars and zirconia mill balls).

The exact amount of alumina powders, 0.4 wt.% TAC and respective amount of deionized water are mixed for 30 min at a speed of 250 rpm. Then the pH is adjusted to about 9.3 with analytical 4.94 N ammonium hydroxide (Aldrich, USA) before adding the exact amount of PAA. The above suspensions are then ball-milled for about 20 min to get the final suspensions. The pH value of the final suspension is 9.0.

4.3. Measurement of the rheological properties

Viscosity is measured using a Modular Compact Rheometer (MCR 300, Paar Physica) with a concentric-cylinder measurement system (CC27), the inner cylinder having a diameter of 27 mm. The temperature ramp rotation measurements are conducted to measure the temperature dependence of suspension viscosity. The shear rate is 20 s^{-1}, and the temperature is raised at a rate of 1 °C/ min. The starting temperature is 25 °C and the final temperature is 85 °C. A total of 60 points is obtained. The temperature dependence of the storage and loss modulus are measured using the temperature ramp oscillation mode with the fixed shear strain amplitude of 1%, frequency of 1 Hz, and the temperature ramp of 1 °C/ min. The starting temperature is 25 °C and the final temperature is 85 °C. A total of 60 points is obtained.

The relative viscosity was computed using the ratio of the measured viscosity to that of the water at the same temperature. A polynomial expression for the temperature dependence of viscosity of water can be fixed to data from the CRC Handbook, as can be shown in the following expression.

$$\eta_{\text{Water}} = 0.0017 - \left(4.73 \times 10^{-5}\right)T + \left(7.45 \times 10^{-7}\right)T^2 \\ - \left(6.25 \times 10^{-9}\right)T^3 + \left(2.13 \times 10^{-11}\right)T^4$$

where T is the temperature of the slurry with a unit of degree centigrade (°C).

5. Results and discussions

5.1. Determination of the strain amplitude for oscillation measurement

Fig. 1 illustrates the results of a typical strain sweep experiment, showing the linear viscoelastic region, i.e. where the storage modulus G' is nearly invariant in the strain and a nonlinear region with decreasing values of G'. It can be seen that 1% strain amplitude is in the linear viscoelastic region at a frequency of 1 Hz. Therefore, 1% strain amplitude is used in the measurements.
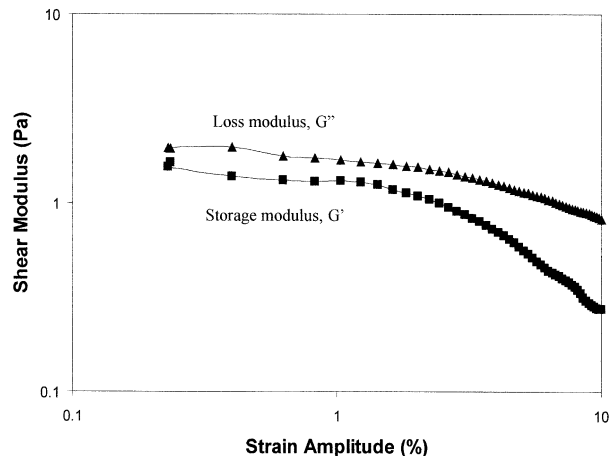

Fig. 1. Variation of shear modulus with strain amplitude for the 40 vol.% AKP53 alumina suspension with 0.4 wt.% TAC and 0.04 wt.% PAA 50,000. The frequency is 1 Hz.

5.2. Determination of the volume fraction threshold, ϕ_g

The volume fraction gelation threshold is the minimum amount of alumina particles required to form a continuous percolation network when the amounts of other components are fixed. Since the basic idea of percolation is the existence of a sharp transition at which the long-range connectivity of the system appears, while this transition occurs abruptly when some generalized density in this system reaches a critical value (percolation threshold). Here we use the temperature dependence of the shear viscosity and shear modulus to find the volume fraction gelation threshold. The variation of the shear modulus can illustrate when the aggregate floc starts to form while the variation of the storage modulus can give an indication when the space-filling particle network will form. Only after the formation of a particle network can the suspension show abrupt change in storage modulus so that the suspension manifest the transition behavior from "fluid-like" to "solid-like", and the storage modulus G' starts to become larger than the loss modulus G''.

Fig. 2 shows the temperature dependence of the relative viscosity under constant shear rate of 20 s^{-1} when the suspension temperature is raised at 1 °C/min. The relative viscosity for the 0.1 volume fraction suspension seems independent of temperature. Whilst the relative viscosity starts to increase above a critical temperature, T_0, when the volume fraction is higher than 0.15. At volume fraction 0.15, the relative viscosity starts to increase sharply at $T_0 \sim 53$ °C first but the increment slows down from about 64 °C. For the suspensions with volume fraction of particles higher than 0.15, the relative viscosity continues increasing sharply. These data indicate that 0.15 might be around the volume fraction gelation threshold, and above this volume fraction the number of alumina particles might be sufficient enough to
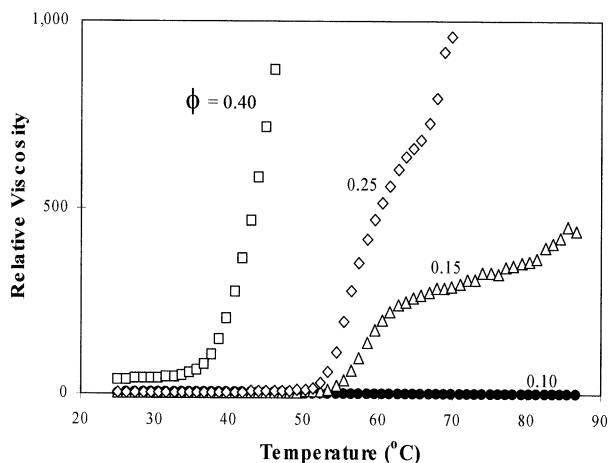
Fig. 2. Variation of the relative viscosity with temperature for different volume fraction particle suspensions with 0.04 wt.% PAA 50,000. The measurements are conducted at a constant shear rate of 20 s⁻¹, and the temperature is raised at a rate of 1 °C/min. The definition of relative viscosity is in the text.

Fig. 3. Temperature and volume fraction dependence of the shear modulus for AKP53 alumina suspensions with 0.04 wt.% PAA of Mw~50,000. The measurements are conducted under 1% strain amplitude and 1 Hz frequency. The temperature is increased at a rate of 1 °C/min.

form a space-filling network in the 0.04 wt.% PAA containing suspension when the temperature is raised. The relative viscosity increase might be due to the bridging agglomerate formation and growth in the suspension. The higher volume fraction of solids will result in higher number density of the aggregate flocs. Furthermore, these flocs will grow with increasing temperature because more and more particles will fill into the interstice of the bridging flocs, and these flocs can connect with each other to form a larger floc. Therefore, the relative viscosity will be further increased. If the volume fraction of solids is small, aggregation flocs will cease to grow when all the particles are located in the flocs and the leveling off occurs for the relative viscosity shown in Fig. 2, e.g. for the 0.15 volume fraction suspension.

Fig. 3 is the temperature dependence of shear modulus for the alumina suspensions with 0.04 wt.% PAA of Mw~50,000. From these curves, we can see that both the storage and the loss modulus do not have an evident change when the volume fraction of particles is 0.1. Starting from 0.15 volume fraction, the storage modulus shows some increase at T'_0 ~70 °C, but the magnitude is rather small. When the volume fraction is above 0.15, all suspensions show significant variation of storage and loss modulus with temperature. It can also be seen that a "crossover" point just appears between the G' and G'' curves when the volume fraction of particles is 0.15, and higher volume fraction particle suspensions show this "crossover" point more clearly. This "crossover" behavior can be a reflection of the occurrence of gelation, or the "transition" from "fluid-like" to "solid-like". This "transition" temperature might be the point where the number density of the bridging flocs is large enough so that the three-dimensional space-filling network (particle percolative network) starts to form.
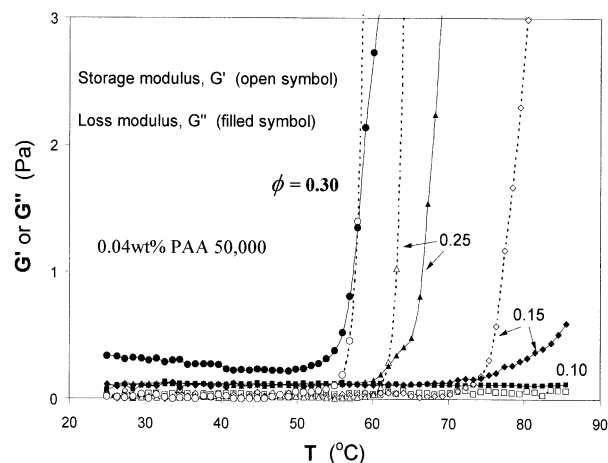
Even though the measurement methods are different and we can not conclude that $T_0 < T'_0$, the data in Figs. 2 and 3 may give an indication of the aggregate growth during this time period or temperature range before a space-filling network could be formed. Therefore, we can draw the conclusion from the above assumptions that the volume fraction of alumina with PAA 50,000 is about 0.15, or ϕ_g ~30.15. We also noticed that in the amount range of PAA in TIF alumina suspensions (<0.5 wt.%), PAA amount will not have a significant effect on the volume fraction gelation threshold of the AKP alumina particles.

Another issue is the variation of the volume fraction gelation threshold with the molecular weight of PAA caused by the difference of the polymer chain length. Similar as the above investigations for the PAA of Mw~50,000 containing suspensions, measurements are conducted for the suspensions with 0.04 wt.% PAA of Mw~10,000 and Mw~5000. Fig. 4 demonstrates the temperature dependence of shear modulus for the 0.04 wt.% PAA 10,000 containing suspensions with variation in the volume fraction of the alumina particles. Using the similar procedures, it can be determined that the volume fraction gelation threshold for the 0.04 wt.% PAA 10,000 containing suspensions is about 0.20, or ϕ_g~0.20. For the 0.04 wt.% PAA (Mw~5000) containing suspensions as shown in Fig. 5, the volume fraction gelation threshold can be taken as ϕ_g~0.35.

Therefore, it seems that for the 0.04 wt.% PAA alumina suspensions, the volume fraction gelation threshold decreases with increasing molecular weight of PAA. This might be due to the longer polymer chain length for the higher molecular weight PAA and the higher possibility of the locally formation of the percolation networks by the stronger interaction between polymer

chains and particles. Therefore, less amount of particles are required to form the percolation network in the suspension with increasing temperature so as to result in the evident change of the shear modulus.

5.3. Determination of the suspension microstructure exponent, s

By taking logarithm to both sides of Eq. (6), we can get

$$\ln G' = s \cdot \ln \left\{ \phi_0 \cdot e^{-\Delta U/kT} \cdot e^{d1 \cdot [d2+(T-T_0)/T_0]} / \phi_g - 1 \right\} + \ln(G'_0) \tag{7}$$

If the above expanded percolation model is a good approximation for the TIF alumina slurries, then
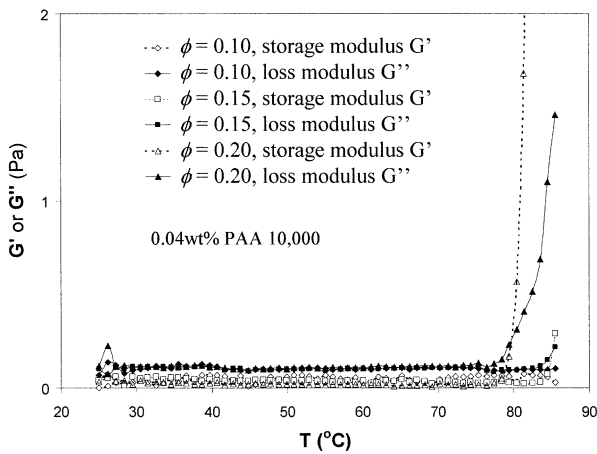
Fig. 4. Temperature and volume fraction dependence of the shear modulus for AKP53 alumina suspensions with 0.04 wt.% PAA of Mw~10,000. The measurements are conducted under 1% strain amplitude and 1Hz frequency. The temperature is increased at a rate of 1 °C/min.
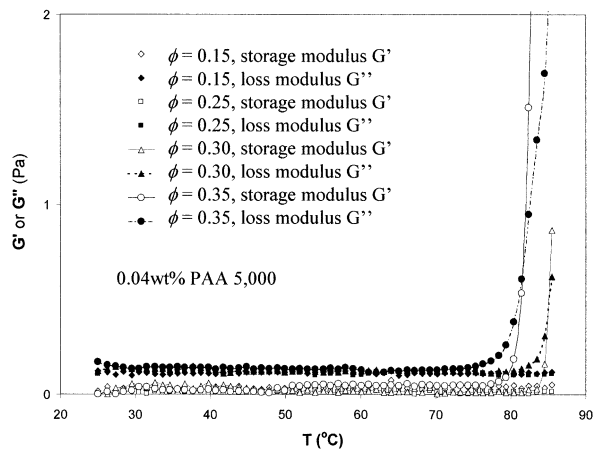
$\ln G' \sim \ln \{ \phi_0 \cdot e^{-\Delta U kT} \cdot e^{d1 \cdot d2 + (T-T_0)} / T_0 / \phi_g - 1 \}$ plot using the experimental data should yield a linear relationship with a slope value of s.

During the calculation, we denote $\ln \{ \phi_0 \cdot e^{-\Delta U kT} \cdot e^{d1 \cdot d2 + (T-T_0)} / T_0 / \phi_g - 1 \}$ as $\ln\{x\}$ for simplicity. The volume fraction of alumina in the suspensions is varied from 0.3 to 0.5 with 0.04 wt.% PAA. G' takes the measured storage modulus value at the same specific temperature as that in $\ln\{x\}$. ϕ_g uses the value obtained and $\phi_g = 0.15$ for 0.04 wt.% PAA of Mw~50,000 alumina suspensions. Fig. 6 gives the results for the 0.04 wt.% PAA of Mw~50,000 containing suspensions while fixing $T_0 = 30$ °C. The value of T_0 can be obtained from the temperature dependence of the relative viscosity of the 40 vol.% alumina suspensions with 0.04 wt.% PAA, where the relative viscosity starts to increase at this temperature as shown in Fig. 2. The variation of T0 with PAA molecular weight is summarized and shown in Table 1. The data points below the line of $\ln G' = 0$ are those that do not fall in the percolative network region because the network does not form yet in the low temperature range for that volume fraction of particles. Therefore, we do not count these points. The points that are far above the line of $\ln G' = 0$ are those where the percolation network has been formed at the respective temperature and volume fraction of particles. These points can be fitted to a straight line with slope of about 4.6 and an intercept of -4.0 in the axis of $\ln G'$ when $\ln\{x\} = 0$. Therefore, we can get $s \sim 4.6$ and $\ln(G'_0) = -4.0$, or $G'_0 \sim 0.02$ Pa.

Similar treatments can be applied to the 0.04 wt.% PAA of Mw~10,000 and Mw~5000 containing alumina suspensions. Fig. 7 shows the determination of the s value for PAA of Mw~5000 containing alumina slurries. These linear characters partially prove that a percolative particle network forms in the TIF alumina
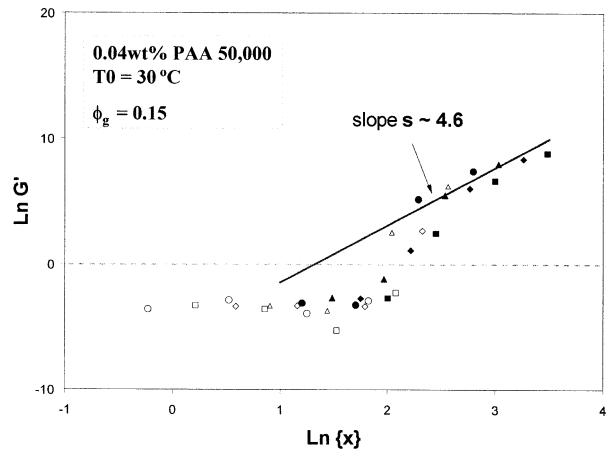
Fig. 5. Temperature and volume fraction dependence of the shear modulus for AKP53 alumina suspensions with 0.04 wt.% PAA of Mw~5000. The measurements are conducted under 1% strain amplitude and 1 Hz frequency. The temperature is increased at a rate of 1 °C/min.

Fig. 6. Exponent s determination for the 0.04 wt.% PAA of Mw~50,000 containing suspensions while fixing $T_0 = 30$ °C. The volume fraction in the suspensions is varied from 0.3 to 0.5. All the measurements are conducted under 1% strain amplitude and 1 Hz frequency. The temperature is increased at a rate of 1 °C/min.

slurries. These results are summarized in Table 1. The data in Table 1 show that the values of all four parameters increase with the decrease of the PAA molecular weight. Large values of s are due to the higher percolative degree of particle networks.[7–11] Smaller s value with respect to the higher molecular weight of PAA reflects the lower percolative nature in the suspensions, which might be a reflection that less particles involve in the "building" of the space-filling network before it forms. The stronger interactions between polymers and particles might be the reason. The larger ϕ_g value for PAA of Mw~5000 containing suspensions also support this conclusion because more particles are involved to form the particle percolation networks instead of the role of the PAA chain/particle interactions. The effect of the magnitude of s on the storage modulus can be shown in Fig. 8 using Eq. (6) for the 40 vol.% alumina suspensions with 0.04 wt.% PAA of Mw~10,000.

The data in Table 1 show that T_0 increases with the decreasing of the PAA molecular weight for the same volume fraction alumina suspensions. This might be attributed to its slower growth rate of the aggregates because the smaller molecular weight PAA chain has less carboxyl groups to connect with particles compared with the larger molecular weight PAA chains at the same temperature. Therefore, there will be larger size aggregate flocs in the higher Mw PAA containing suspensions than

that of the lower Mw PAA containing suspensions so that the relative viscosity of the former suspension may start to increase at a relatively lower temperature.

Effect of the amount of PAA on the value of s is also studied. The results shown in Fig. 9 indicate that the s value decreases to ~4 for the 0.5 wt.% PAA 50,000 containing suspensions compared with that of the 0.04 wt.% PAA 50,000 suspensions. The value of G'_0 increases by more than five times from ~0.02 to ~0.12

Table 1
Effect of PAA molecular weight on the parameters in Eq. (6)

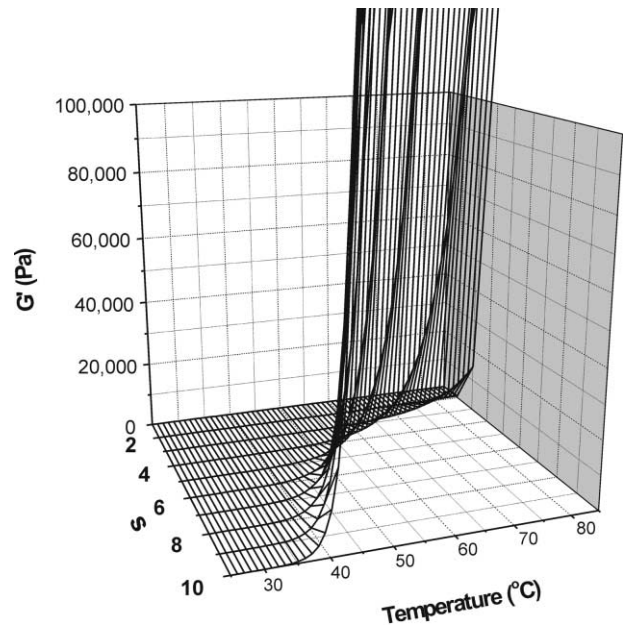|	PAA Mw~50,000	PAA Mw~10,000	PAA Mw~5000
s	~4.5	~5.5	~6.0
G'_0	~0.02 Pa	~0.57 Pa	~33 Pa
ϕ_g	~0.15	~0.20	~0.35
T_0	~30 °C	~40 °C	~50 °C

Fig. 8. Variation of the storage modulus with exponent s and temperature calculated by model Eq. (6) for 0.04 wt.% PAA (Mw ~10,000) containing alumina TIF suspensions. The parameters are $\phi = 0.40$, $d1 = 1.3$, $d2 = 0.1$, $\Delta U = -5$ eV, $G_0 = 0.57$, $\phi_g = 0.20$ and $T_0 = 40$ °C.
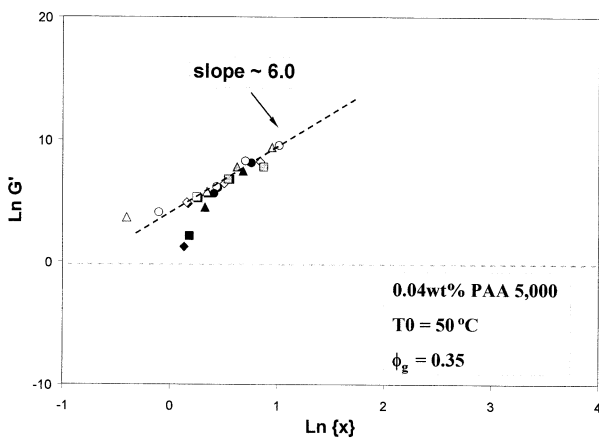

Fig. 7. Exponent s determination for the 0.5 wt.% PAA of Mw~5000 containing suspensions while fixing $T_0 = 30$ °C. The volume fraction in the suspensions is varied from 0.3 to 0.5. All the measurements are conducted under 1% strain amplitude and 1 Hz frequency. The temperature is increased at a rate of 1 °C/min.
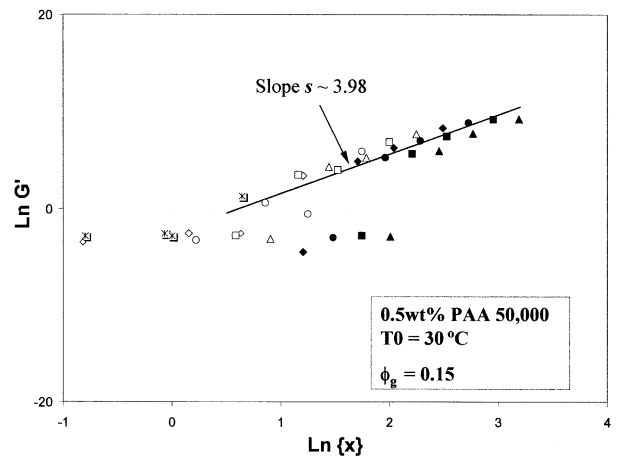

Fig. 9. Exponent s determination for the 0.5 wt.% PAA of Mw~50,000 containing suspensions while fixing $T_0 = 30$ °C. The volume fraction in the suspensions is varied from 0.3 to 0.5. All the measurements are conducted under 1% strain amplitude and 1 Hz frequency. The temperature is increased at a rate of 1 °C/min.

Pa. Therefore, the value of G'_0 increases with the amount of PAA in the suspensions, but the percolation network nature decreases with the increment of PAA amount, which is reflected by the decrease of the value of s.

5.4. Comparison of the calculated and measurement results

Fig. 10 shows both the calculated results using Eq. (6) and the measurement data for the 0.04 wt.% PAA (Mw~50,000) containing alumina suspensions. The volume fraction of particles for each suspension is 0.3, 0.4 and 0.5, respectively. The parameters shown in Table 1 are used for calculations. We can see that the
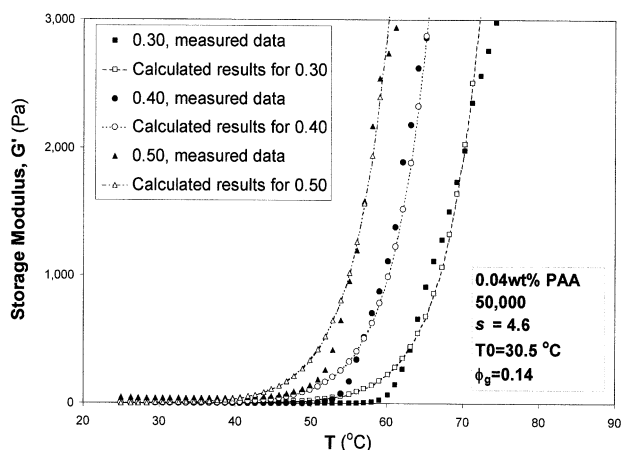

Fig. 10. Comparison of the calculation results using Eq. (6) and the measurement data for the 0.04 wt.% PAA (Mw~50,000) containing alumina suspensions with volume fraction of particles 0.3, 0.4 and 0.5, respectively. The measurements are conducted under 1% strain amplitude and 1 Hz frequency. The temperature is increased at a rate of 1 °C/min.
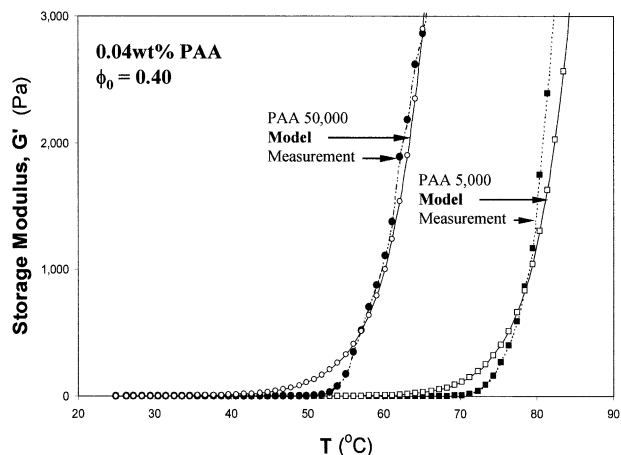

Fig. 11. Comparison of the calculation results using Eq. (6) and the measurement data for the 0.04 wt.% PAA (Mw~50,000 and 5000) containing alumina suspensions with 0.40 volume fraction of particles. The measurements are conducted under 1% strain amplitude and 1 Hz frequency. The temperature is increased at a rate of 1 °C/min.

calculated results are in good agreement with the measurement data for all solid-loading suspensions especially in the high temperature range. Fig. 11 illustrates that our percolation model also applies to all molecular weight PAA containing alumina suspensions at a solid loading of 40 vol.%. Therefore, we can draw a conclusion that our expanded percolation model reflects the intrinsic nature of the evolution of the microstructure for the TIF alumina suspension to some extent.

6. Summary

We first introduce the concept of "effective volume fraction of aggregates", ϕ_{eff}, and propose a continuous percolation theory model to interpret the evolution of the storage modulus with temperature and solid loading for the TIF alumina suspensions. The exponent, s and the volume fraction gelation threshold, ϕ_g are derived from experimental data. The magnitude of ϕ_g increases with the PAA molecular weight. The percolative degree increases with the decreasing of the PAA molecular weight, which is reflected by the higher value of s. The calculated results using our expanded percolation model and the experimental-derived parameters are in good agreement with the measurement data. This model applies to all solid loading and all molecular weight PAA containing TIF alumina suspensions well.

References

1. Lange, F. F., Powder processing science and technology for increased reliability. *J. Am. Ceram. Soc.*, 1989, **72**, 3–15.
2. Horn, R. G., Surface forces and their action in ceramic materials. *J. Am. Ceram. Soc.*, 1990, **73**, 1117–1135.
3. Sigmund, W. M., Bell, N. S. and Bergström, L., Novel powder processing methods for advanced ceramics. *J. Am. Ceram. Soc.*, 2000, **83**, 1557–1574.
4. Aldinger, F., Sigmund, W. M. and Yanez, J., Formgebungs methode für Keramiken und Metalle in Wässrigen Systemen mittels Temperaturänderung. German Pat. No. 197 51 696.3, 1998.

5. Bell, N. S., Wang, L., Sigmund, W. M. and Aldinger, F., Temperature induced forming: application of bridging flocculation to near-net shape production of ceramic parts. *Z. Metallkd.*, 1996, **90**, 388–392.

6. Stoll, S. and Buffle, J., Computer simulation of bridging flocculation processes: the role of colloid to polymer concentration ratio on aggregation kinetics. *J. Colloid Interf. Sci.*, 1996, **180**, 548–563.

7. Bergström, L., Shear thinning and shear thickening of concentrated ceramic suspensions. *Colloids and Surfaces, A: Physicochemical and Engineering Aspects*, 1998, **133**, 151–155.

8. Bremer, L. G. B., Bijsterbosch, B. H., Schrijvers, R., van Vliet, T. and Walstra, P., On the fractal nature of the structure of acid casein gels. *Colloids Surf.*, 1990, **51**, 159–170.

9. Hentschel, H. G. E., Fractal dimension of generalized diffusion-limited aggregates. *Phys. Rev. Lett.*, 1984, **52**, 212–215.

10. Wolthers, W., van den Ende, D., Breedveld, V., Duits, M. H. G., Potanin, A. A., Wientjes, R. H. W. and Mellema, J., Linear viscoelastic behavior of aggregated colloidal dispersions. *Physical Review E*, 1997, **56**, 5726–5731.

11. Rueb, C. J. and Zukoski, C. F., Viscoelastic properties of colloidal gels. *J. Rheol.*, 1997, **41**, 197–218.

12. Stauffer, D., *Introduction to Percolation Theory*. Taylor & Friends, London, 1985 pp. 1–50.

13. Yanez, J. A., Larrz, E. and Bergström, L., Viscoelastic properties of particle gels. *J. Colloid Interface Sci.*, 1999, **209**, 162–172.

14. Feng, S. and Sen, P. N., Percolation on elastic networks: new exponents and threshold. *Phys. Rev. Lett.*, 1984, **52**, 216–219.

15. Yanez, J. A., Shikata, T., Lange, F. F. and Pearson, D. S., Shear modulus and yield stress measurements of attractive alumina particle networks in aqueous slurries. *J. Am. Ceram. Soc.*, 1996, **79**, 2917–2924.

16. Sonntag, R. C. and Russel, W. B., Elastic properties of flocculated networks. *J. Colloid. Interf. Sci.*, 1987, **116**, 485–489.

17. Shih, W. H., Shih, W. Y., Kim, S. I., Liu, J. and Aksay, I. A., Scaling behavior of the elastic properties of colloidal gels. *Phys. Rev. A*, 1990, **42**, 4772–4779.

18. Buscall, R., Mills, P. D., Goodwin, J. W. and Lawson, D. W., Scaling behavior of the rheology of aggregate networks formed from colloidal particles. *J. Chem. Soc., Faraday Trans. 1*, 1988, **84**, 4249–4260.

19. Málek, J., Mitsuhashi, T. and Criado, J. M., Kinetic analysis of solid-state processes. *J. Mater. Res.*, 2001, **16**, 1862–1871.

20. Yang, Y. and Sigmund, W. M., Rheological properties, gelation diagram and direct casting process of the temperature induced forming (TIF) alumina suspensions. *J. Mater. Synthesis Process*, 2001, **9**, 103–109.

21. Yang, Y. and Sigmund, W. M., Effect of volume fraction of particles on the viscoelastic properties of the temperature induced forming (TIF) alumina suspensions. *J. Am. Ceram. Soc.*, 2001, **84**, 2138–2140.